Journal of Cardiothoracic Surgery

RESEARCH

Open Access

MRI in the prenatal genetic diagnosis and intrauterine treatment of fetal congenital cystic adenoma of the lung

Xiaolin Hou[1], Mei Yu[1], Ying Liu[2*] and Liwei Yan[3]

Abstract

Objective To investigate the value of magnetic resonance examination technique for prenatal genetic diagnosis and clinical intrauterine treatment of fetal congenital cystic adenoma (CCAM) of the lung.

Methods A retrospective analysis was conducted on 108 pregnant women admitted to a certain hospital from January 2016 to January 2022 for pre natal examination and consultation on eugenics. The selected pregnant women were aged 20–40 and had a gestational age of 17–36 weeks. Ultrasound and MRI examinations were performed on 108 pregnant women who met the inclusion criteria. Follow-up and investigation were conducted on the fetus after being diagnosed with CCAM. To analyze the results of prenatal genetic diagnosis, chromosome microarray analysis (CMA) was used to analyze samples with pathogenic Copy Number Variants (CNV) and identify pathogenic genes. Finally, the imaging diagnosis results obtained through statistical software were analyzed, and the correlation between pathogenic genes and CCAM, as well as the clinical application value of MRI in fetal intrauterine treatment was explored.

Results Among all cases, 68 fetuses were diagnosed with CCAM through ultrasound examination; 71 fetuses were diagnosed with CCAM through MRI examination. A total of 74 samples were confirmed as CCAM by autopsy and neonatal CT. The sensitivity, specificity, and accuracy of MRI in diagnosing fetal congenital CCAM were higher than those of ultrasound examination. The expression of CCAM was positively correlated with DUSP22, PRSS1, and SHOX, with all R values greater than 0.8. The clinical decision curve showed that when the probability of fetal CCAM was less than 0.03, the prenatal genetic diagnostic model of MRI was not applicable; But when the probability of fetal CCAM was higher than 0.05, the auxiliary intrauterine treatment effect that MRI diagnostic methods achieved was significantly better than conventional diagnosis.

Conclusion MRI is significantly better than ultrasound in the diagnosis of CCAM, which can effectively improve the sensitivity of diagnosis and provide accurate information for the eugenics of pregnant women, and has high clinical application value.

Keywords MRI examination, CCAM, Diagnosis, Treatment, Genetics

*Correspondence:
Ying Liu
liuyingyisheng@163.com
Full list of author information is available at the end of the article

Background

Congenital Cystic Adenoma of the lung (CCAM) is a relatively rare form of bronchiectasis, accounting for approximately one quarter of the incidence of congenital lung disease in fetuses. The main pathological feature of CCAM is the abnormal development of air bubbles in the lungs and the adenomatous appearance of the terminal bronchi [1, 2]. Three types of CCAM (type I, type II and type III) have long been classified from a clinical and pathological point of view and are still used today. The management and treatment of CCAM varies according to the type of fetal oedema and the occurrence of comorbidities such as mediastinal deviation, making CCAM typing important for the assessment of fetal clinical pregnancy outcome [3, 4]. The early and accurate diagnosis of fetal CCAM, the evaluation of the severity of the disease, and the provision of appropriate advice and measures are essential for the eugenics of the pregnancy [5, 6]. The study retrospectively analyzed the clinical data of 108 pregnant women who underwent antenatal MRI and were successfully followed up until the birth of their son, and collected all the data generated during the process in order to provide a clinical reference for prenatal genetic diagnosis and intrauterine treatment of CCAM by MRI.

Methods

General information

All 108 cases of pregnant women admitted to a certain hospital for antenatal check-ups and eugenic counselling from January 2016 to January 2022 were collected as the study population. The age distribution of the selected pregnant women ranged from 20 to 40 years old, and their gestational age ranged from 17 to 36 weeks. Certain principles of inclusion and exclusion were followed in the selection of the study population. Patient inclusion criteria: (1) pregnant women with 18 to 26 weeks of menopause; (2) no contraindications to any ultrasound examination; (3) complete clinical data; (4) clear maternal last menstrual period; (5) no maternal syndrome during pregnancy; (6) no maternal history of alcoholism or smoking; (7) intact fetal membranes; (8) understanding of the advantages and disadvantages of participating in this study, willing to cooperate with all hospital examinations and signing an informed (8) understood the advantages and disadvantages of participating in the study, were willing to cooperate with all hospital investigations and signed an informed consent form. Exclusion criteria: (1) patients who did not meet the above requirements; (2) patients with incomplete medical records containing metallic foreign bodies; (3) patients with immune system disorders and claustrophobic pregnant women; (4) patients who were unable to co-operate with the doctor in completing the relevant investigations or to complete the follow-up; (5) patients who withdrew from the experiment. Patients are explained in detail throughout the experiment and are instructed to sign an informed consent form after obtaining their consent, which is strictly approved by our hospital's ethics committee. The experiment was conducted on the basis of ethical principles.

Research methodology

Ultrasound and MRI were performed on all 108 pregnant women who met the entry criteria. All pregnant women who underwent ultrasound underwent a comprehensive special examination of the fetal chest to determine whether the fetus had congenital cystic adenoma-like disease. The confirmed cases were followed up with MRI and the corresponding pregnancy outcome and child status were recorded.

Ultrasonography

The ultrasound equipment used was a Siemens G60S Doppler ultrasound diagnostic device and the abdominal probe was selected to suit the size of the patient. A 3.5 MHz abdominal probe was used for normal sized patients and a 2-5 MHz abdominal probe was used for fatter sized patients. During the examination, the pregnant woman was selected in the supine position and scanned in multiple views for careful observation of the fetus [7, 8]. If a lesion was found in the lung, the location, size and internal echogenicity of the lesion should be observed in multiple views and directions, and colour Doppler ultrasound should be used to observe the haematological status of the lesion and the relationship of the surrounding great vessels to see if pleural fluid and other abnormalities are present [9]. If a pregnant woman had a genetic abnormality, it must be ensured that the pregnant woman does not have other chest abnormalities before undergoing an ultrasound examination.

Ultrasound examination operators all hold corresponding medical imaging professional qualification certificates, proving that they have the professional ability to perform ultrasonic examinations. All ultrasound operators were professionally trained radiologists, prenatal diagnosticians, or medical experts with relevant professional backgrounds. Complex fetal lesions, such as congenital pulmonary cystadenoma, required operators to have a high degree of diagnostic ability and a deep understanding of ultrasound images.

MRI examinations

A GE Signa HDx 1.5 T superconducting MRI scanner was used to perform abdominal MRI on all participating pregnant women, using an 8-channel body coil as the transmitting and receiving coil, in the supine position with the foot extended forward. The fetus was scanned

in sagittal, axial and coronal positions with TR3.6 ms, TE1.7 ms, FOV42cmX42cm, layer thickness 5 mm and layer spacing 1 mm. The number of layers scanned by the instrument was determined by the extent of the scan. The results of the scan were read by two experienced radiologists and important information about the fetus such as the signal and location of the lesion was clarified and determined whether it was a CCAM of the fetus [10].

Computed tomography (CT) examination of the newborn

When the median CT dose index volume (CTDIvol) was large, the resulting larger CTDIvol meant a higher radiation dose, which will increase potential long-term health risks, such as an increased risk of cancer, which is detrimental to the growth of the fetus and pregnant women. of health. Therefore, all pregnant women participating in the experiment underwent low-dose CT examination after giving birth to their newborns to diagnose whether the newborns had congenital pulmonary cystadenomatous malformations.A GE 128-layer spiral CT machine was used, set up with a scan thickness of 2 cm, a pitch of 1 cm, a voltage of 120 kV and automatic milliamps (30-40mas). A CT scan of the fetus's chest was performed followed by an enhanced scan. A high pressure injection was also used to inject the contrast agent iopamidol at a rate of 1 ml per second (the dose was based on 2 ml per kg). Two experienced radiologists determined the CT images and the enhanced images and clarified important information about the fetus such as the signal and location of the lesion and whether it is a congenital cystic adenomatoid malformation of the fetus [11]. An example of CCAM classification is shown in Fig. 1.

Follow-up and examination of the fetus after diagnosis

If the fetuses were diagnosed with CCAM after MRI, the doctor should promptly explain to the mother and their family the prognosis of the fetus and after asking the family's opinion, advise them to induce labour. If the fetus was not oedematous, the mother might be advised to consider continuing the pregnancy depending on the actual condition. Ultrasound examinations were repeated every fortnight to monitor the development of the lesion.

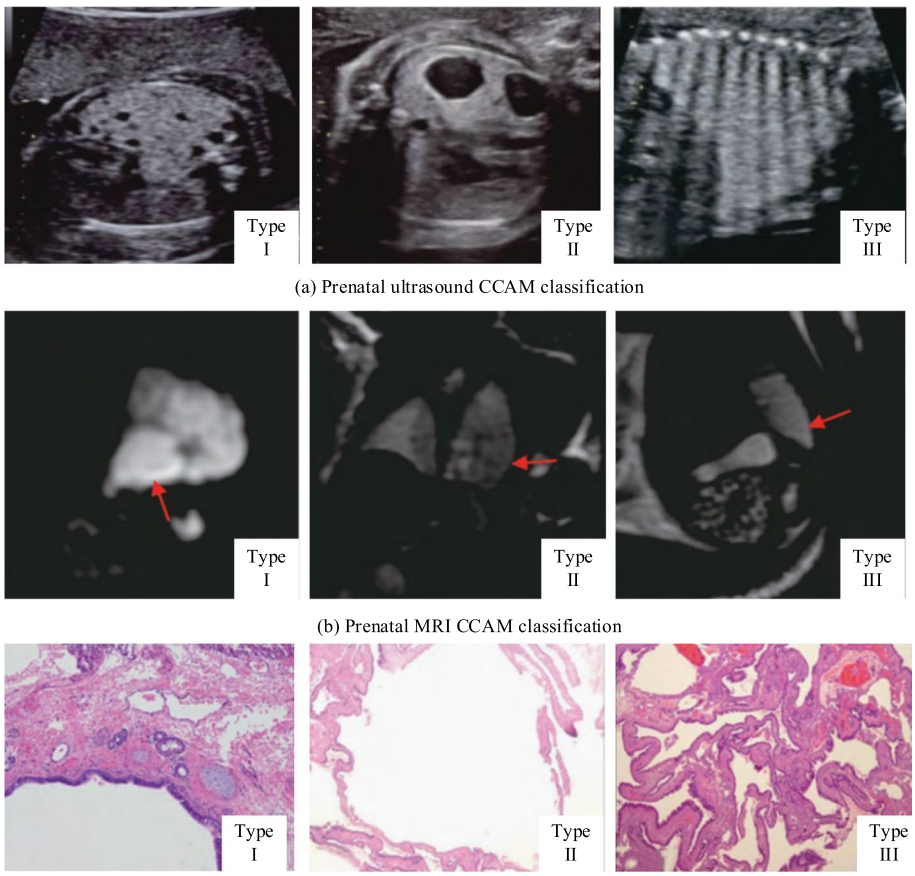

Fig. 1 CCAM classification

If the fetus developed a mediastinal shift, microcystic pattern, or suspected airway obstruction during follow-up if the gestational week was at less than 32 weeks, prompt intervention should be made. Alternatively, hormonal therapy, cystic shunt puncture or open fetal surgery might be used to restore the outcome and physiology of the fetal lung to promote fetal lung development, depending on the actual condition of the fetus and the mother. After 32 weeks of gestation, if there were no clinically significant symptoms, the woman might continue to be observed and have a spontaneous delivery. If during follow-up after 32 weeks of gestation the fetus developed a significant mediastinal shift, microcystic pattern or suspected airway obstruction, early caesarean section was recommended. If floaters or enlargement were found, emergency surgery on the fetus to further relieve the occupying lesion was required at the same time as the caesarean section was performed [12]. After 32 weeks of gestation, if the fetus had significant oedema or a large occupying lesion that makes delivery via natural delivery difficult, an immediate caesarean section should be performed and emergency surgery on the fetus should be performed after delivery.

Chromosome microarray analysis (CMA) and analysis of CMA results

The whole genomic DNA of the children was analyzed and processed using the CytoScan microarray kit provided by Affymetrix. Genomic DNA digestion, ligation, amplification, purification, fragmentation, labelling of signals, hybridisation and washing of the microarray, scanning and data analysis were carried out in strict accordance with the standard experimental procedures provided by Affymetix [13]. The samples with pathogenic Copy Number Variants (CNV) were also analysed by CMA technique to determine the pathogenicity gene.

Statistical methods

All data were processed with SPSS 22.0 statistical software and Kappa values were used for consistency testing. Diagnostic differences between MRI findings and pathological findings were compared. For measurement data, the mean ± standard deviation was used to express the difference, and for comparison between two groups, the t-test was used. For analysis of diagnostic indicators, a four-compartment table was used to calculate the difference, with $P<0.05$ indicating a statistically significant difference.

Results

Clinical case characteristics of the patient

Among the 225 pregnant women admitted to a certain hospital for antenatal check-ups from January 2016 to January 2022, there were 108 cases of children with CCAM. The general clinical data of all children are shown in Table 1, which shows that of the 108 children with CCAM, 55 were male and 53 were female. The left and right side of the lesion was found in 82 and 26 children respectively. Concomitant conditions were defined as a combination of other abnormalities on ultrasound in addition to CCAM. All selected children had concomitant CCAM and the MRI images were observed by two radiologists with many years of medical experience. There was no significant difference between the sex and number of cases of all children.

Analysis of pregnancy outcomes

A total of 108 pregnant women were diagnosed, 68 with CCAM on ultrasound and 71 with CCAM on MRI. 51 of these women were diagnosed with CCAM on ultrasound and MRI and were induced after meeting the characteristics of induction of labour. Pregnant women diagnosed with CCAM by ultrasound and MRI were continuously monitored and examined every fortnight to keep abreast of the changes in the condition of the children.

Factors influencing pregnancy outcomes

The study proposed to divide the children with CCAM into two groups, namely the induction and delivery groups, corresponding to the case and control groups

Table 1 Analysis of general clinical data of children with CCAM

Initial gestational age	Number of cases	Gender		Lesion site		Accompanying situation		Constituent ratio/%
		Male	Female	Left	Right	Have	Nothing	
< 24	41	23	18	32	9	13	28	37.96
24–28	53	25	28	40	13	13	40	49.07
28–32	6	3	3	5	2	4	2	5.55
Postpartum	5	3	2	3	9	1	4	4.63
Unknown	3	1	2	2	1	1	2	2.78
Total	108	55	53	82	26	32	76	100

Table 2 Logistic regression analysis of pregnancy outcomes in pregnant women with CCAM

variable	B	S.E	Wald	df	Sig	Exp(B)
Constant term	-3.435	1.280	7.26	1	0.007	0.032
Residence	1.468	0.725	4.698	1	0.043	4.342
History of poor fertility	1.966	1.239	2.592	1	0.107	7.357
exceptional case	1.584	0.702	5.089	1	0.024	4.873

A characteristic condition is an ultrasound indication of an abnormality other than an occupying lung lesion

Table 3 CCAM typing by different means of diagnosis

	CCAM category	Number of cases	Constituent ratio (%)
US	Type I	21	30.88
	Type II	28	41.18
	Type III	19	27.94
	total	68	100
MRI diagnosis	CCAM category	Number of cases	Constituent ratio (%)
	Type I	21	29.58
	Type II	29	40.85
	Type III	21	29.58
	total	71	100

Table 4 Diagnosis of CCAM by induction of labour pathology and neonatal CT

Prenatal imaging diagnosis results		Induced abortion pathology and neonatal CT diagnosis results		Total
		Positive	Negative	
US	Positive	46	28	74
	Negative	22	12	34
	Total	68	40	108
MRI	Positive	53	21	74
	Negative	18	16	34
	Total	71	37	108

respectively, in order to observe their effect on pregnancy outcome in children with CCAM. A multifactorial logistic regression analysis was carried out to screen the variables by likelihood ratios by relating maternal age, place of residence, occupation, history of adverse births, number of pregnancies and whether the fetus was combined with hydrothorax to the pregnancy outcome of the children with CCAM. Table 2 shows that among the six factors, the three factors of maternal residence, history of adverse births and special circumstances were statistically significantly different ($p<0.05$); the ORs for the three factors were 4.342, 7.357 and 4.873, respectively. The absence of other co-morbidities was a significant protective factor for live birth delivery of children with CCAM.

MRI versus ultrasonography for CCAM staging (prenatal MRI findings)

The results are shown in Table 3. 68 cases of fetal CCAM were diagnosed by ultrasound, of which 21, 28 and 19 were type I, II and III respectively, accounting for 30.88%, 41.18% and 27.94% respectively. 71 cases of fetal CCAM were diagnosed by MRI, of which 21, 29 and 21 were type I, II and III respectively, accounting for 29.58%, 40.85% and 29.58% respectively. The percentage of fetuses with CCAM diagnosed by MRI was 71, of which 21, 29 and 21 cases were type I, II and III respectively, accounting for 29.58%, 40.85% and 29.58% respectively.

Table 5 Specificity, sensitivity and accuracy of ultrasound and MRI in the diagnosis of CCAM

Imaging methods	Sensitivity	Specificity	Accuracy	Kappa value
US	67.68	98.54	97.35	0.85
MRI	75.12	98.94	98.18	0.89
x^2	5.482	0.789	1.374	-
P	0.016	0.217	0.082	-

Diagnosis of CCAM by pathology of induced labour and neonatal CT

The diagnosis of CCAM was analyzed using the induction pathology and neonatal CT findings as the gold standard. The results of which are shown in Table 4. 74 samples were diagnosed with CCAM confirmed by autopsy and neonatal CT.

Specificity, sensitivity and accuracy of ultrasound and MRI in the diagnosis of CCAM

The specificity, sensitivity and accuracy of ultrasound and MRI in the diagnosis of CCAM were statistically analyzed using the gold standard of induction of labour pathology and neonatal CT diagnosis, and the results are shown in Table 5.

Follow-up results of children after birth

Of the 108 pregnancies, 51 were induced and 57 were live births. 57 children with CCAM were delivered live, 7 were delivered with extra-uterine management, 2 were delivered live with open surgery and 48 were referred to the neonatal unit for neonatal pneumonia, with an average length of stay of (16 ± 14) days. All live births were followed up postnatally. 18 fetuses were not examined regularly for pulmonary masses; 10 fetuses had regular CT examinations, which showed a significant reduction in pulmonary masses after birth; 20 fetuses had pulmonary masses removed immediately after birth; 7 fetuses were managed outside the uterus at delivery; the remaining 2 fetuses were operated on at delivery, and CT examinations showed that there were no significant differences in weight, growth and height in 57 cases compared to normal children of the same age.

Analysis of CMA results

Due to the overall length of time the samples were kept (2016 to 2022), environmental factors such as temperature and humidity resulted in some samples having unusable DNA. Ultimately, 44 usable samples were obtained out of the 51 samples of children with induced labour, and the resulting samples were further analyzed by chromosomal microarray. In this study, CT was performed on the newborns after delivery of the pregnant women, and the diagnosis of CCAM was eventually confirmed in 7 cases, and a total of 37 cases of CCAM were actually included after exclusion of the diagnosis. A total of 258 CNVs (100 microdeletions and 158 microduplicated fragments) were detected, with fragment sizes ranging from 100 Kb to 6.72 MB, of which 241 fragments ranged from 100 Kb to 1 Mb and 17 fragments were larger than 1 Mb. Of these, 241 fragments were between 100 Kb and 1 Mb and 17 fragments were greater than 1 Mb, of which 11 fragments were pseudochimeric. Three cases of pathogenic microdeletions/microduplications were detected in the CMV fragments, including a 1.60 MB microdeletion in the critical region of 17q12 (34,822,465–36,418,529) for RCAD syndrome (sample p7235), a 1.40 MB microdeletion in the critical region of 17p12 (14,087,933–15484358) for HNPP syndrome (Sample A10757), 17p12 (14,087,787–15441802) microduplication of 1.35 MB in the critical region of CMT1A syndrome (Sample A15554). Based on the MRI diagnostic results, Affymetrix cell suspension hd arrays were performed on three fetuses using the CMA technique, and the results are shown in Fig. 1. In Fig. 1, clear pathogenic CNV fragments were detected in all three fetuses, and the overall detection rate of pathogenic CNV was 8.2% (Fig. 2).

Based on these results, it was hypothesised that recurrent CNV fragments in multiple samples were associated with fetal CCAM disease. Of the 258 fragments detected, 177 fragments co-occurred in more than 2 fragments (actually 23 fragments in common). Of these 23 fragments, 20 were polymorphic and the remaining 3 contained pathogenic genes (9 samples). It was therefore hypothesized that the candidate pathogenic genes for fetal CCAM were more likely to be present in these

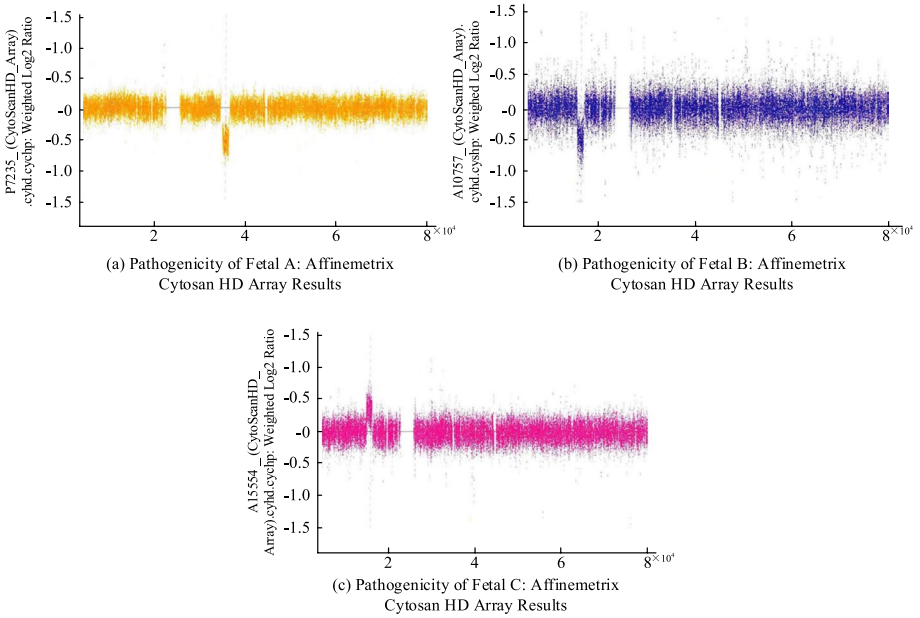

(a) Pathogenicity of Fetal A: Affinemetrix Cytosan HD Array Results

(b) Pathogenicity of Fetal B: Affinemetrix Cytosan HD Array Results

(c) Pathogenicity of Fetal C: Affinemetrix Cytosan HD Array Results

Fig. 2 Analysis of fetal CMA results

3 fragments, and that the DUSP22, PRSS1 and SHOX genes in these fragments might be candidates for fetal CCAM lesions.

Correlation analysis between CCAM and pathogenic genes.

To test the experimental hypothesis, the correlation between the DUSP22, PRSS1, SHOX genes and CCAM expression in the CNV fragment was continued to be explored, and the specific results are shown in Fig. 3. Figure 3(a) shows the results of the correlation analysis between CCAM and DUSP22. The expression of CCAM disease showed a significant positive correlation with the DUSP22 gene, and the R value was calculated. Figure 3(b) shows the correlation between CCAM and PRSS1 gene, with a moderately concentrated scatter distribution and a calculated R value of 0.804. Figure 3(c) shows the correlation between CCAM and SHOX gene, with a more concentrated scatter and an R value of 0.812. In summary, the correlation between CCAM and the three genes were all positive, with R values greater than 0.8.

To further enhance the diagnostic capability of the MRI imaging histology model, the study combined the three genes to construct a column line graph model, and the results are shown in Fig. 4, with the red dots in Fig. 4 indicating cases. Figure 4(a) shows the diagnostic probability of DUSP22 gene expression. By combining the fetal DUSP22 gene, pregnancy cycle and MRI imaging label, the probability of DUSP22 expression in the child was 0.712. Figure 4(b) shows the diagnostic probability of PRSS1 gene expression. By analyzing the PRSS1 level in the child, pregnancy cycle and imaging label, the probability of PRSS1 expression in the child could be obtained. Figure 4(c) shows the diagnostic probability of positive SHOX gene expression in a child with CCAM, with a probability of 0.721 for the combination of SHOX gene level, pregnancy cycle and imaging label.

Calibration curve analysis was then used to validate the fit of the column line plot in the application of prenatal genetic diagnosis of fetal CCAM, as shown in Fig. 4. In Fig. 4, there was a small difference between the column line plot diagnostic and actual values for the joint assessment in the diagnosis of CCAM-DUSP22 gene expression status prediction, and the p-value for comparing the predicted results of the joint assessment in CCAM-DUSP22 expression status with the actual observed genetic risk was 0.534, which was not a statistically significant difference. The diagnostic curve of the column line plot for the combined assessment in the diagnosis of CCAM-PRSS1 expression status was the most closely matched to the actual values, with a *P-value* of 0.839

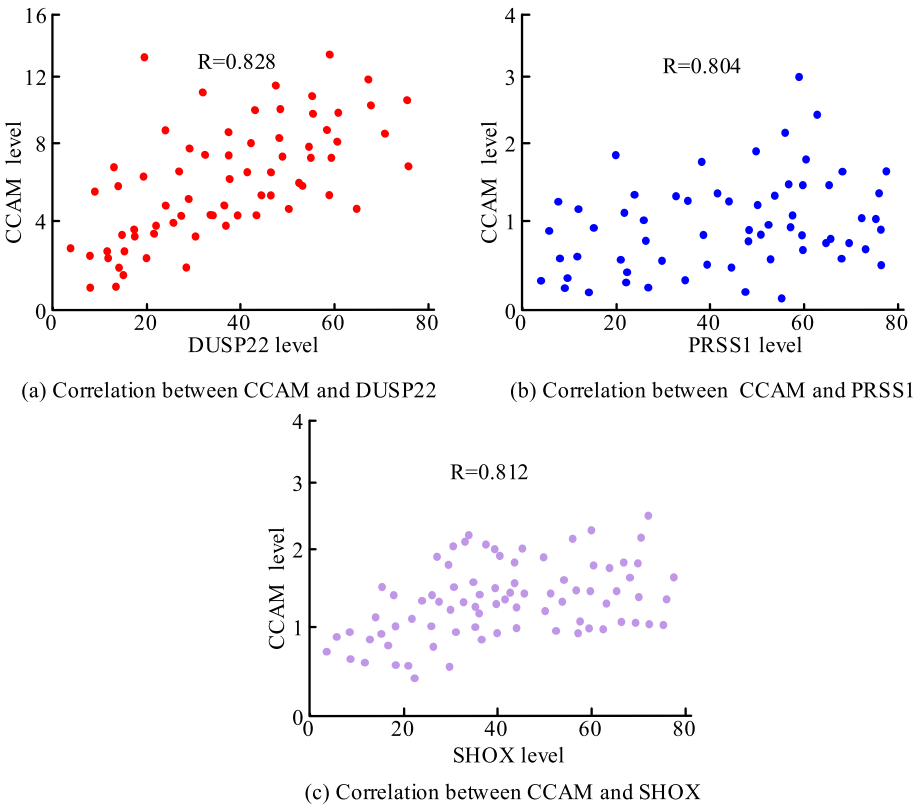

Fig. 3 Correlation analysis of DUSP22, PRSS1 and SHOX genes with CCAM expression

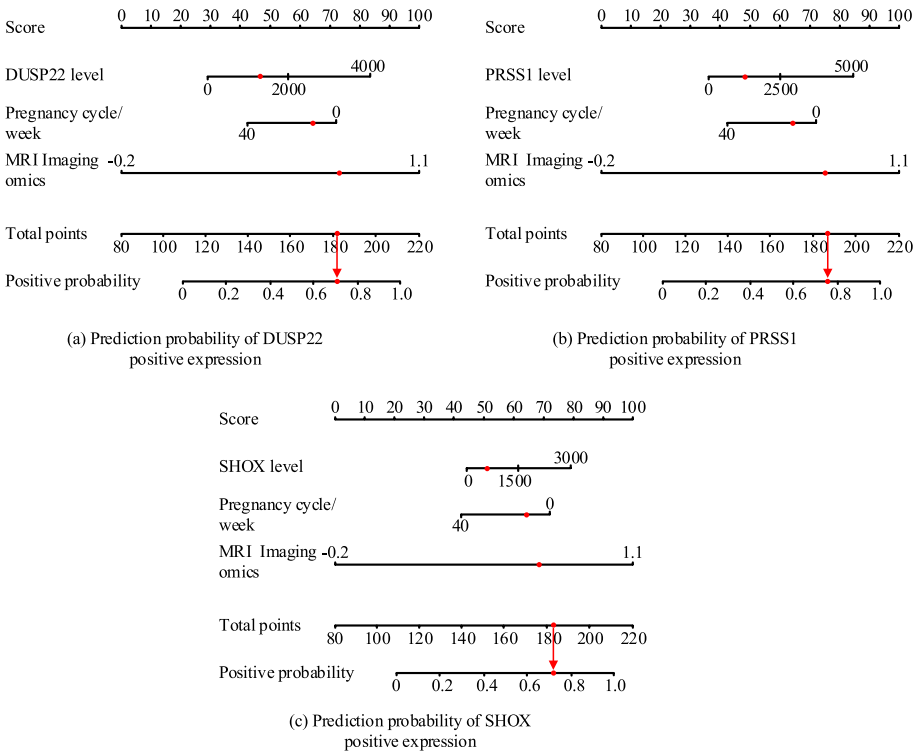

Fig. 4 Diagnostic risk line graph prediction

shown between the risk diagnosis and the actual results, a statistically significant difference. The joint assessment in the diagnosis of CCAM-SHOX expression status showed the greatest fit between the diagnostic curve of the column line graph and the actual value, with a *P value* of 0.798 shown between the risk diagnosis and the actual value (Fig. 5).

Analysis of clinical therapeutic value

The clinical decision curve was then used to analyse the clinical treatment value of MRI applied to the diagnosis of CCAM disease, as shown in Fig. 6. In Fig. 6, clinical diagnostic interventions were defined as routine diagnoses for all children followed up, and no interventions were considered not to have been performed for any children. The DUSP22 expression status co-assessment diagnosis, the PRSS1 expression status co-assessment diagnosis and the SHOX expression status co-assessment diagnosis were evaluated for children with CCAM. It was found that the MRI prenatal genetic model for the three genes was not applicable when the fetal risk of CCAM was below 0.03; however, when the fetal risk of CCAM was significantly higher than 0.05, the MRI diagnostic tool was able to achieve a much higher treatment effect than the conventional diagnosis.

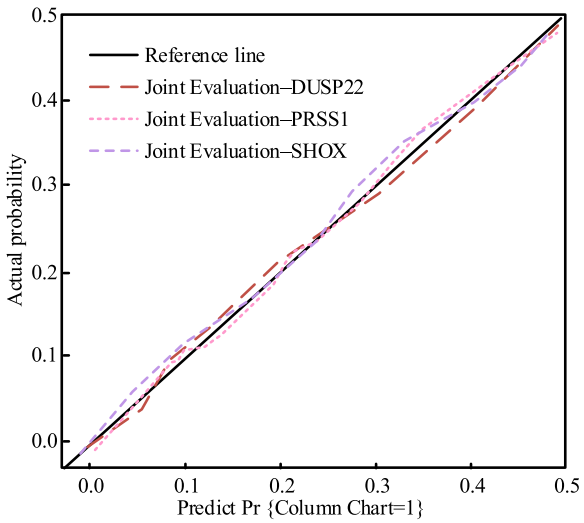

Fig. 5 Fit analysis of the MRI combined diagnostic model

Discussion

The safety and health of the fetus are the two most important points for pregnant women and their families during the perinatal period. With the advancement of various perinatal technologies, genetic counselling and eugenics are gradually seeping into the minds of

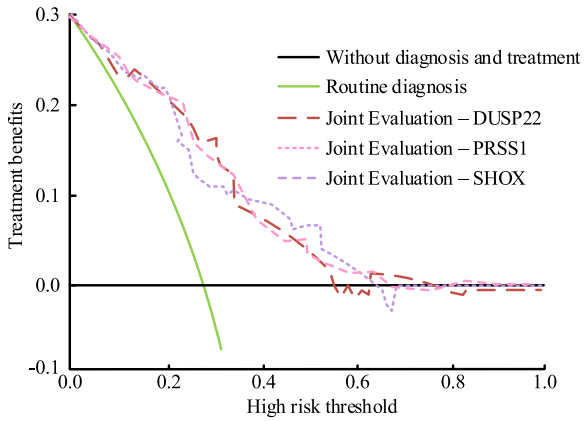

Fig. 6 Clinical decision curve

prospective parents. In recent years, the detection rate of abnormal fetal lung development has been increasing year by year, with CCAM being the most prominent type of fetal congenital lung disease [14, 15]. The pathogenesis of CCAM is unclear, and the following elements are currently clear for CCAM. First, CCAM has a high incidence at 7–10 weeks of embryonic formation, during which the abnormal value-added of the fetal terminal fine bronchi is evident, inhibiting the growth rate of fetal lung air bubbles and leading to a disorder in the development of fetal bronchial structures, preventing the normal development of alveoli. Second, some clinical studies have suggested that the etiology of CCAM may be related to individual pathogenic gene fragments, but the available studies do not support the conclusion of the above view. Thirdly, the incidence and detection rate of fetal congenital CCAM varies between countries, regions and hospitals. Accurate antenatal screening and diagnosis of the fetus is essential, and the previous form of antenatal screening for fetal CCAM was ultrasonography (i.e. ultrasound). Most CCAM disorders can be diagnosed by ultrasound, but the results of ultrasound examination of the fetal chest cavity vary from one pregnant woman to another and have limitations that affect the diagnostic accuracy of ultrasound [16, 17]. At the same time, ultrasound requires a high level of technical skills and the ability to discriminate between ultrasound images.

Magnetic resonance technology (MRI) has the characteristics of high-resolution imaging, which can compare small molecules such as proteins and nucleic acids in liquids and living bodies without destroying the cells being examined, and analyse their molecular structures, thus enabling the differentiation between normal and abnormal tissues [18, 19]. MRI can show different tissues very well, and can also show abnormal structures in the same tissues, so that MRI can be used to differentiate between normal and abnormal tissues for disease diagnosis [20, 21]. In addition, MRI can also achieve multimodality imaging in multiple planes with a large field of view, which can visualize the blood circulation and structural status around the lesion and better reflect the specific situation of the lesion, thus reducing the difficulty for the physician to read the film [22, 23]. Compared with ultrasound, MRI can provide more useful information in showing fetal chest abnormalities, such as CCAM, BPS, congenital diaphragmatic hernia, etc., especially when the ultrasound image is unclear or the diagnosis is uncertain. This shows that MRI can provide clearer soft tissue contrast and a more comprehensive anatomical view, helping to identify the exact location, size and shape of the lesion.

Currently, Ultrasound(US) and Magnetic Resonance Imaging (MRI) play a very important role in the prenatal diagnosis process of fetal congenital cystic adenoma (CCAM). These imaging technologies can be used to detect and characterize structural abnormalities in the fetus, allowing efficient genetic evaluation based on fetal abnormality. Based on this, the experiment used ultrasound and MRI to perform prenatal genetic diagnosis of CCAM on the same group of pregnant women. During the process, the fetuses were treated with different methods of intrauterine treatment based on the imaging results to explore the practical application effect of MRI. Based on the follow-up results obtained, the pregnant women and their families were advised to take appropriate treatment and management measures in order to achieve a good pregnancy outcome and fetal prognosis.

Intrauterine surgical treatment mainly includes intrapartum extrauterine fetal surgery and open fetal surgery. Intrauterine surgical treatment is mainly to control the continued development of pathological changes in fetal tissues and organs, improve their functions, gain time and create conditions for fetal development and maturity. The indications for 108 fetuses to undergo MRI examinations were mainly potential or suspected congenital cystadenomas (CCAM) and other fetal structural abnormalities discovered during prenatal ultrasound examination, which required further detailed evaluation to confirm the diagnosis and formulate treatment. Prenatal ultrasound examination of all fetuses revealed that 68 fetuses had characteristic manifestations of CCAM, such as cystic or solid masses in the lungs and possible mediastinal shift. MRI and CT examinations were performed on all patients, and it was found that 71 and 74 fetuses had characteristic manifestations of CCAM respectively.

To clarify the effect of three pathogenic genes, DUSP22, PRSS1 and SHOX, on CCAM disease, different diagnostic models of gene expression were constructed using MRI images. The results showed

a positive correlation between CCAM and the three genes, with all R-values greater than 0.8. To further improve the diagnostic ability of MRI images, a line graph model was constructed combining fetal pathogenic genes, pregnancy cycle and MRI images, which showed that the probability of expression of the three genes exceeded 0.7, indicating the ability of MRI to discriminate between genes. The results showed that when the probability of fetal CCAM was less than 0.03, the prenatal genetic diagnosis model of MRI was not applicable. However, when the probability of fetal CCAM was higher than 0.05, MRI diagnostic tools could obtain significantly better adjunctive treatment than conventional diagnosis.

Conclusion

In summary, the diagnostic effect of MRI on fetal congenital CCAM is significantly better than that of ultrasound examination, and it can effectively improve the sensitivity, specificity and accuracy of diagnosis. Fetal MRI has higher resolution and is not limited by fetal position. It can detect lesions that cannot be detected by ultrasound to a certain extent and judge the severity of fetal disease, which has high clinical application value. Although MRI itself does not provide genetic information, it can display fetal anatomical abnormalities in detail. This information can help doctors evaluate the severity and extent of CCAM, and is crucial for genetic counseling and further genetic testing. MRI findings can also be used to predict fetal prognosis, including the need for treatment after birth. For example, the size and type of CCAM shown on MRI and whether it is accompanied by other structural abnormalities can help predict respiratory function and surgical risks in the neonatal period. In summary, although MRI is not directly related to genetic diagnosis or intrauterine treatment, the anatomical information it provides is of great value for genetic risk assessment, intrauterine treatment decision-making, prognosis judgment, and the development of management plans.

However, MRI examination also has certain limitations, including higher equipment and technical requirements, and higher examination costs, so it may not be as universally accessible as ultrasound examination. In addition, the MRI examination process is relatively time-consuming and may not be as convenient as ultrasound examination for rapid evaluation and screening. There are also certain requirements for pregnant women's body shape, amniotic fluid volume, fetal position, etc. These factors may affect the quality of the image and the accuracy of diagnosis.

Acknowledgements
Not applicable.

Authors' contributions
XH, MY, YL and LY participated the search and collection data, drafting of the manuscript; study concept and design, study supervision. All authors read and approved the final manuscript.

Funding
The research is supported by: 2021 Hebei medical science research project plan (No. 20211366); 2007 Hebei science and technology support project plan (No. 072761740).

Availability of data and materials
The original contributions presented in the study are included in the article.

Declarations

Ethics approval and consent to participate
The study was approved by the local ethics committee of the Hebei Medical University. All experiments were performed in accordance with relevant guidelines and regulations such as the Declaration of Helsinki and the patients signed the informed consent form and agreed to be published.

Consent for publication
Not applicable.

Competing interests
The authors declare no competing interests.

Author details
[1]Prenatal Diagnosis Center, The Fourth Hospital of Shijiazhuang (The Obstetrics and Gynecology Hospital of Hebei Medical University), Shijiazhuang, Hebei, China. [2]Obstetrical Department VIII, The Fourth Hospital of Shijiazhaung (The Obstetrics and Gynecology Hospital of Hebei Medical University), Shijiazhuang, Hebei, China. [3]Neonatal Surgery, The Fourth Hospital of Shijiazhuang (The Obstetrics and Gynecology Hospital of Hebei Medical University), Shijiazhuang, Hebei, China.

Received: 23 March 2024 Accepted: 14 June 2024
Published online: 28 August 2024

References

1. Ruiz M, Wilson MP, Randhawa S, Low G. Incidental maternal findings on fetal MRI. Clin Radiol. 2023;78(5):356–61.
2. Bourgioti C, Konidari M, Gourtsoyianni S, Moulopoulos LA. Imaging during pregnancy: what the radiologist needs to know. Diagn Interv Imaging. 2021;102(10):593–603.
3. Shahab S, Fangusaro J. Neonatal central nervous system tumors. Clin Perinatol. 2021;48(1):35–51.
4. Bekiesińska-Figatowska M. Editorial for " 3D Volumetric MRI Detects Early Alterations of the Brain Growth in Fetuses with Congenital Heart Disease." J Magn Reson Imaging. 2021;54(1):273–4.
5. Green DB, Wallace AB, Restrepo CS, Merrick DT, Raptis DA, Bhalla S, Vargas D. Fluid-filled cystic lesions of the lungs. J Thorac Imaging. 2021;36(4):208–17.
6. Karaosmanoglu AD, Arslan S, Akata D, Ozmen M, Haliloglu M, Oguz B, Karcaaltincaba M. Congenital and hereditary cystic diseases of the abdomen. Insights Imaging. 2020;11(1):1–19.
7. Armutlu A, Quigley B, Choi H, Basturk O, Akkas G, Pehlivanoglu B, Adsay NV. Hepatic Cysts: Reappraisal of the Classification, Terminology. Am J Surg Pathol. 2022;46(9):1219–33.
8. El Ammar F, Bulwa ZB. Neurology of Systemic Disease: Selected Topics with a Focus on Women. Neurol Clin. 2023;41(2):399–413.
9. Revzin MV, Moshiri M, Katz DS, Pellerito JS, Mankowski Gettle L, Menias CO. Imaging evaluation of fallopian tubes and related disease: a primer. Radiographics. 2020;40(5):1473–501.
10. Harun N, Alanin M C, Collins L H C, Hopkins C, Odell E W. The 7th Annual Scientific Meeting, International Academy of Pathology, Malaysian Division Kuantan 2021: Dermatopathology, Uropathology and Gynaecologic

pathology was held virtually on 5th-7th March 2021. Abstracts of paper (poster) presented are as follows. Malays J Pathol. 2021;43(3):465–501.
11. Samejima K, Takai Y, Matsunaga S, Nagai T, Kikuchi A. The safety and effectiveness of elective laparoscopic surgery for benign ovarian cysts during pregnancy-Comparison with emergency surgery. Journal of Obstetrics and Gynaecology Research. 2022;48(10):2603–9.
12. Kim HHR, Hull NC, Lee EY, Phillips GS. Pediatric Abdominal Masses: Imaging Guidelines and Recommendations. Radiologic Clinics. 2022;60(1):113–29.
13. Chalard F, Hermann A L, Elmaleh-Bergès M, Ducou le Pointe H. Imaging of parotid anomalies in infants and children. Insights into imaging. 2022;13(1):1–19.
14. Sun L, Amerom J, Marini D, Portnoy S, Seed M. Characterization of hemodynamic patterns in human fetuses with cyanotic congenital heart disease. Ultrasound Obstet Gynecol. 2021;58(6):824–36.
15. Sarma A, Heck JM, Ndolo J, Newton A, Pruthi S. Magnetic resonance imaging of the brainstem in children, part 1: imaging techniques, embryology. Pediatr Radiol. 2021;51(2):172–88.
16. Castro P T, Matos A P, Werner H, Lopes, J, Ribeiro G, & EA Júnior. Evaluation of fetal nasal cavity in bilateral congenital dacryocystocele: 3D reconstruction and virtual navigation by magnetic resonance imaging. Ultrasound in Obstetrics & Gynecology. 2020;55(1):141–3.
17. Peyvandi S, Rollins C. Fetal Brain Development in Congenital Heart Disease. Can J Cardiol. 2023;39(2):115–22.
18. Ren JY, Zhu M, Dong SZ. Three-Dimensional Volumetric Magnetic Resonance Imaging Detects Early Alterations of the Brain Growth in Fetuses With. J Magn Reson Imaging. 2021;54(1):263–72.
19. Maduram A, Farid N, Rakow-Penner R, Ghassemi N, Pretorius DH. Fetal Ultrasound and Magnetic Resonance Imaging Findings in Suspected Septo-Optic Dysplasia. J Ultrasound Med. 2020;39(8):1601–14.
20. Castro PT, Fazecas T, Matos A, Ribeiro G, Júnior EA, Werner H. Concomitant fetal duodenal and esophageal atresia three-dimensional reconstruction from magnetic resonance imaging. Ultrasound Obstet Gynecol. 2022;59(2):277–8.
21. Nishida K, Fujioka K, Sugioka Y, Abe S, Morioka I. Prediction of Neurodevelopmental Impairment in Congenital Cytomegalovirus Infection by. Neonatology. 2020;117(4):460–6.
22. Li Z, Lv YD, Fang R, Li X, Zhu L. Usefulness of prenatal magnetic resonance imaging in differential diagnosis of fetal congenital cystic adenomatoid malformation and bronchopulmonary sequestration. World J Clin Cases. 2021;9(4):822–9.
23. Akuma AO, Okoye AG. The outcome of fetuses diagnosed with congenital cystic adenomatous malformation of the lungs: Experience of a regional neonatal center (2004–2016). Journal of Clinical Neonatology. 2020;9(3):189.

Publisher's Note